

# A new adaptive filter and quality evaluation index for image restoration

A.R. Jiménez, R. Ceres and J.L. Pons  
Instituto de Automática Industrial (CSIC)  
Ctr. Campo Real, Km. 0.2 La Poveda  
28500 Arganda del Rey, Madrid, Spain  
Phone: 34 918 711 900 Fax: 34 918 717 050  
e-mail: arjimenez@iai.csic.es  
<http://www.iai.csic.es/lopsi>

## Summary

A new technique for image adaptive restoration called  $3\sigma$ -MPF and the *GRI* index, which evaluates the restoration performance of smoothing methods, are presented in this paper.

The  $3\sigma$ -MPF restoration method (*3 $\sigma$ -Multiresolution Plane Fitting*) performs a plane fitting with variable-sized windows over continuous regions or applies the *MTM* (Modified Trimmed Mean) filter when discontinuities are detected. The criteria used to control the window size and to detect discontinuities is the *3 $\sigma$ -fidelity* test. The use of this filter is especially appropriate when the restored image is desired to have high smoothing over continuous regions (noise-free) and it is important to preserve significant patterns in the image (no deformations).

Additionally, the paper presents a Global Restoration Index called *GRI*. The *GRI* index allow the evaluation of any restoration technique and is defined by integrating two basic indices which measure in an independent manner the smoothness and fidelity of the restoration. Using the *GRI* index, the  $3\sigma$ -MPF filter performance is compared with other methods mentioned in the literature. Our filter obtains an outstanding performance under gaussian noise degradation and also is robust against outliers. Since the authors are involved in the processing of range images for spherical object detection, the restoration of range images is used as an example of the excellent results obtained when applying the  $3\sigma$ -MPF filter.

## Abstract

This paper presents a new technique for image adaptive restoration called  $3\sigma$ -MPF and the *GRI* index, which evaluates the restoration performance of smoothing methods. The  $3\sigma$ -MPF filter is based on an adaptive plane fitting technique using variable-sized windows with different behavior for continuous regions or discontinuities. The criteria used to select the window size and detect discontinuities is the *3 $\sigma$ -fidelity* test. The Global Restoration Index, *GRI*, integrates two independent indices measuring restoration smoothness and fidelity. Using this index, the  $3\sigma$ -MPF filter performance is compared with other traditional methods, demonstrating better performance under gaussian noise and robustness against outliers.

## keywords:

restoration, smoothing, adaptive filter, evaluation index, filter performance comparison.

# 1 Introduction

The presence of noise in images is a major problem that typically negatively affects image analysis and interpretation processes. Therefore, to improve the performance of higher level processing stages, a filtering method has to be applied in order to reduce noise and consequently to obtain a better estimate of the ideal image. The techniques used to fulfill this requirement are known as *restoration methods* and have been studied for years, with a long history of research, not only within the image processing community but also in the signal processing field.

Assuming an ideal image model which consists of a set of continuous smooth regions surrounded by discontinuities connecting the different regions, and considering a degraded image that contains additive noise with gaussian, uniform or impulsive distribution, the purposes of image restoration are to:

- *Remove the noise (Smoothness).* A restoration method must eliminate the noise disturbing the image to recover the original smoothness of each continuous region. Therefore, every region, regardless of being curved or flat, must be transformed into a smooth surface as our image model states.
- *Preserve discontinuities (Fidelity).* The discontinuities are preserved and there should not be any deformation of the image, providing an estimate with high fidelity or similarity in terms of absolute deviation between the ideal and the restored image.

For restoring an image there are four main filter categories: *linear*, *non-linear*, *adaptive* and *iterative* methods. The *linear* filters can be applied in the spatial or Fourier domain and some of the most representative are the gaussian filter, the arithmetic mean, specific-designed FIR (Finite Impulse Response) filters, the inverse and the Wiener filter<sup>(1)</sup>. The *non-linear* family includes order statistic filters such as the median, trimmed mean and mid-range filters<sup>(2)</sup>; morphological filters such as gray-level erosion, dilatation, opening and closing operators; homomorphic and hysteresis filters; non-linear mean filters such as the harmonic mean, contra-harmonic mean,  $Y_p$  mean and geometric mean<sup>(3)</sup>, as well as other techniques such as wavelet de-noising<sup>(4)</sup> and neural network filtering<sup>(5,6)</sup>.

The *adaptive* method applies both linear and non-linear algorithms but are mainly characterized by a filter parameter adjustment depending on the local features detected over each particular location on the image, for example, local noise variance or the presence of discontinuities. These filters are appropriate when both smoothing and discontinuity preservation objectives are desired. The CDOR (Contrast Dependent Outlier removal)<sup>(1)</sup> is an adaptive filter that uses center-deleted estimates for adaptive tuning and is comparable to the median filter for outlier removal. Other classical filters are the sigma filter<sup>(7)</sup>, the gradient inverse weight method (GIW), the selected neighbourhood mean filter (SNA)<sup>(3)</sup>, the minimum square mean error filter (MSME)<sup>(8,9)</sup> and the scale-space smoothing technique<sup>(10)</sup>. Experiments performed by Lee demonstrated that the sigma filter performs better against gaussian noise than the GIW, median and SNA filters. This fact has also been observed by our team using the GRI index as will be discussed later in this paper.

The MAS filter (Multiresolution adaptive smoothing)<sup>(11)</sup> is another adaptive method that works by searching for the biggest window that contains a flat and constant region. The criteria used to detect this region is based on the comparison of a local and global homogeneity measurement. In the case that the window is declared homogenous, the estimated value of the central pixel will be the window mean. When no homogeneous region is detected, i.e when trying to estimate over a pixel which is close to a discontinuity, a MSME filter is applied to preserve this discontinuity.

The MAS filter is then compared with other iterative methods previously presented by Saint-Marc and Perona<sup>(12,13)</sup>, concluding by visual criteria that the MAS method performs better than the others. In spite of this result, we consider the MAS method to present some limitations since there is no smoothing of pixels close to discontinuities because the MSME filter applied in these cases does not smooth in the proximity of discontinuities. Additionally, the MAS filter smoothes very poorly when surfaces are not constant, i.e. in regions where there are slopes. A sloped region in the image has a significant local variance, and therefore the filter reacts reducing the window size because it is designed to avoid averaging on discontinuities. A smaller window size implies an estimation with lower smoothing since the pixels in the window to be averaged are less.

The DW-MTM filter (Double Window-Modified Trimmed Mean)<sup>(14)</sup>, which is a modification of the trimmed mean filter, was designed to overcome the problems of the MMSE filter to remove impulse noise. Using a small window, a reference value is obtained by means of the median filter. Then, this reference is used by the Modified Trimmed Mean (MTM) to average the points lying inside a symmetric interval surrounding the reference. The size of the interval is a parameter which has to be adjusted and is usually  $\pm 2$  or  $\pm 3$  times the estimated noise variance.

The final group of filters are those which work in an *iterative* way. Some representative examples of these filters are the smoothing based on the facet model by Haralick and Watson<sup>(15)</sup>, the variable weight mask presented by Saint-Marc<sup>(16)</sup>, the RESC (Residual Consensus) method that performs random surface fits<sup>(17)</sup> and the heat diffusion based techniques of Trucco<sup>(18)</sup>, Perona<sup>(13)</sup> and Umasuthan<sup>(19)</sup>. These methods usually perform better than the non-iterative versions, but are not useful for applications where a good time response is critical because iteration over an entire image is a highly time-consuming task.

In this paper we propose a non-iterative adaptive filtering method,  $3\sigma$ -MPF, which will be evaluated and compared with several non-iterative techniques, showing that the proposed filter performs better than the others for gaussian noise and is also robust against impulsive noise. The  $3\sigma$ -MPF filter is an improved version of the MAS and DW-MTM filters, retaining their best features, and removing the weak factors, which were overcome by adding a new fidelity test strategy based on a plane fitting procedure. The following three sections present a) the new adaptive filter  $3\sigma$ -MPF, b) the new *GRI* index for restoration evaluation and c) a restoration performance comparison between several techniques using the *GRI* index.

## 2 The new $3\sigma$ -MPF adaptive filter

Most filters in the spatial domain use a reduced processing window to perform a convolution operation. For an adaptive behavior, this convolution window must change in accordance with the features found in the image such as discontinuities or noise. There are two main problems when designing this kind of filter:

1. How to detect the discontinuities.
2. How to select the size of the processing window.

Most of the restoration algorithms perform a comparison between a local variance and a global noise variance. When the local variance is lower or equal to the global noise variance it is assumed that there is no discontinuity and the filter smoothes the image's region, otherwise a discontinuity preserving filter has to be applied over that area. This method is recognized not to be absolutely reliable since the size of the window to compute a local variance has a

severe influence on the final statistic estimation. When using a large window, the discontinuity detection is worse since the influence of pixels over discontinuities does not significantly affect the final variance estimation, although the smoothness obtained is better. However, a small window works better at detecting discontinuities, but does not accomplish sufficient smoothing. Additionally, a surface with a certain slope, which has a higher local variance than a flat one, force the adaptive filter to act as if it were over a discontinuity, therefore there is almost no smoothing performed over these continuous sloped surfaces.

We propose a fitting evaluation criteria, called  $3\sigma$ -*fidelity*, for solving the problem of determining the optimal window size and detecting the presence of each discontinuity. This strategy is based on the residuals obtained from a least-square fitting using a plane. When fitting a plane to the data in a region, we call this fit  $3\sigma$ -*fidelity* if every residual in the fitting region is lower than  $3\sigma$ . This criterion can be defined formally by the following expression:

$$3\sigma\text{-fidelity} = \begin{cases} 1 & \text{If } \forall (x, y) \in v_{ij} \ |g(x, y) - (ax + by + c)| \leq 3\sigma \\ 0 & \text{Otherwise} \end{cases} \quad (1)$$

where  $\sigma$  is the expected noise standard deviation,  $(a, b, c)$  are the three constants that define the fitted plane,  $g$  is the degraded image and  $v_{ij}$  is a region around the  $(i, j)$  pixel which defines the fitting region. The  $a$ ,  $b$  and  $c$  plane parameters are obtained by the following least-square algorithm:

$$a = \frac{\sum_{(x,y) \in v_{ij}} (x - i) \cdot g(x, y)}{\sum_{(x,y) \in v_{ij}} (x - i)^2} \quad (2)$$

$$b = \frac{\sum_{(x,y) \in v_{ij}} (y - j) \cdot g(x, y)}{\sum_{(x,y) \in v_{ij}} (y - j)^2} \quad (3)$$

$$c = \frac{\sum_{(x,y) \in v_{ij}} g(x, y)}{\sum_{(x,y) \in v_{ij}} 1} \quad (4)$$

A discontinuity will be detected when, using a  $3 \times 3$  window as the testing region, the  $3\sigma$ -*fidelity* test is false. When there is no discontinuity, the size of the processing window will be the largest one which fulfills the  $3\sigma$ -*fidelity* test. In this way, we are demonstrating how to design an adaptive filter which can obtain high smoothing ratios and at the same time assures that the maximum distortion factor will be limited.

The  $3\sigma$ -*MPF* filter receives this name because it is based on a multiresolution plane fitting (MPF) which is guided by the  $3\sigma$ -*fidelity* criteria. The filter requires the computation of a noise estimate which is needed to compute the fidelity test. This estimation can be performed using different approaches such as the one presented by Meer for the MAS filter<sup>(11)</sup>. The algorithm begins performing a sequential  $3\sigma$ -*fidelity* test with  $7 \times 7$ ,  $5 \times 5$  and  $3 \times 3$  windows until the first fit satisfying this condition is obtained. Then, the estimation for each pixel is just the  $c$  parameter of the fitted plane, where  $c$  represents the mean window value. If the  $3\sigma$ -*fidelity* test fails using the three windows, then it is assumed that a discontinuity or an impulse exists, and in this case, a discontinuity preserving method with outlier rejection is applied. The filter used under these circumstances is a variation of the Modified Trimmed Mean (MTM) algorithm. A reference value is estimated computing the median of a  $3 \times 3$  window with 4-connectivity, and the mean value around this reference is computed with only pixels inside a  $\pm 3\sigma$  range for a  $3 \times 3$  window with 8-connectivity. For more details, the  $3\sigma$ -*MPF* pseudocode is shown in figure 1.

The filter performs as much smoothing as possible when it finds continuous region without outliers, when a discontinuity is detected it averages only the pixels that belongs to one region, and when outliers are present the average is obtained using the non-outlier's neighbours in the same region. By definition, for gaussian noise and in the worst case, this filter can not generate distortions larger than  $3\sigma$  and the residuals between the ideal and restored images are always below  $6\sigma$ . The smoothing step will be performed with the biggest window size even for sloped surfaces, avoiding the problem other filters have when using local window variance estimation such as the MAS filter. Consequently, this filter smoothes surfaces, preserves discontinuities, does not deform images, and can be applied to plane and curved surfaces at different orientations without any restriction while rejecting outlier noise.

Although, the  $3\sigma$ -MPF filter is a general purpose filter and is ideal for the majority of restoration cases, it also presents two main limitations. The first limitation is that it is more time-consuming than other non-iterative filters since it requires the computation of an important number of fits to a plane ( $N \times N$  in the best case and  $3 \times N \times N$  in the worst case; where  $N \times N$  is the number of pixels in the image). The second limitation is related to the restoration of images containing important rugosity information. This filter assumes an ideal model for the reference image that consist of a set of continuous and smooth surfaces separated by discontinuities. Then the filter tries to transform a noisy image into one similar to the reference model, i.e. smooth regions and well-preserved edges between these continuous regions. But, if our ideal image has a rugosity component on the surfaces that is important to preserve for a specific application, and the image is restored using the  $3\sigma$ -MPF filter, the rugosity will disappear from the surfaces obtaining smooth regions. In fact, this limitation is not exclusive to our method and most of the filters quoted previously assume the same model, and therefore perform in a similar manner when rugosity is important.

In order to get a first visual impression of how this filter works, we have prepared a synthetic image that contain four flat square regions separated by step discontinuities and degraded by gaussian noise, outliers and a combination of both noises (figure 2). The left side shows the three synthetic degraded images and the right side the restored images obtained applying the  $3\sigma$ -MPF filter. It must be noticed that the reconstructions obtained are characterized by a high discontinuity preservation with a substantial smoothing over the continuous regions.

These filtering techniques are being developed and applied in the research being carried out for the automatic harvesting of fruits using specific robot solutions and a laser range-finder perception<sup>(20,21)</sup>. A restoration sample of a real range image that contains a 20 by 20 cm orange tree area including two oranges and several leaves is also presented (figure 3). The left column display, from top to bottom, the noisy range mesh, the gray level version with a horizontal line and the range profile in *mm* corresponding to the selected horizontal line. This noisy range image has additive gaussian degradation that can disturb tasks such as an orange detection process. On the right column, the same information is shown, but after applying our  $3\sigma$ -MPF filter. It must be noted that the representative shapes are conserved, preserving discontinuities and smoothing continuous surfaces without adding absolute errors in range data. The adaptive filter behavior is represented by the masks shown in figure 4. This figure displays, from left to right and top to bottom, the position where estimation was performed using a  $7 \times 7$ ,  $5 \times 5$ ,  $3 \times 3$  averaging or a MTM filter, respectively. In this particular example, the percentage obtained is 17% for the  $7 \times 7$  case, 16% for  $5 \times 5$ , 28% for  $3 \times 3$  windows, and in 39% of the image pixels the MTM filter was applied. That is to say, 33% of the pixels received a special treatment and were smoothed with larger windows than in the traditional case, which uses  $3 \times 3$  windows.

### 3 The GRI index: A restoration quality index for filter evaluation

In the computer vision literature, as shown in the introduction, are a large number of references presenting different restoration techniques. For practical applications, it is useful to apply one of the best restoration techniques to simplify the complexity and performance of further higher level interpretation stages. Therefore it is necessary to have an objective method able to detect which restoration technique performs better than others. Among the techniques used to make comparisons the following ones are highlighted:

- *Visual evaluation.* This method is subjective and can be used when the difference between restorations is obvious. In general, it is not a good method for restoration evaluation and should be restricted only when evaluating enhancement techniques which basically intend to increase the visual quality.
- *Visual evaluation after a processing step.* This technique uses a processing step such as edge detection or transformation to a Hough parameter space to highlight some features in the image. In this way, the visual evaluation is improved since most of the non-distinctive information is removed. However the restoration technique selected with this method depends on the processing stage used for the evaluation and therefore is only optimal for an application which uses this processing step.
- *Quantitative indices.* The most frequently used indices are the mean squared error (5) and the mean absolute error. Other known indices are the cross correlation, the relative mean error, the Strehl factor<sup>(1)</sup> and the mean normal difference (6)<sup>(19)</sup>.

$$e = \frac{\sum_i \sum_j \{f(i, j) - \hat{f}(i, j)\}^2}{\sum_i \sum_j 1} \quad (5)$$

$$d\alpha = \frac{\sum_i \sum_j |\arccos(\vec{n}_f \cdot \vec{n}_{\hat{f}})|}{\sum_i \sum_j 1} \quad (6)$$

The objective in restoration is to obtain an image estimation  $\hat{f}$  as similar as possible to the ideal image  $f$ ; it means that the pixel to pixel distance must be minimized and smoothness in the continuous regions must be maximized. The Strehl and cross-correlation indices measure the reduction in contrast and the proximity between the ideal and estimated images, respectively. The mean squared (5) or absolute error measure the pixel to pixel deviation between both images, however it does not take into account the existence of surfaces with rugosity and it generates the same mean error in surfaces with equal pixel to pixel residuals but with different degrees of smoothing. For capturing the smoothness supplied by the restoration method the mean normal difference index (6) could be used. However, if the discontinuities are not well preserved this metric introduces a large penalty because of the loss of parallelism between the ideal and restored images. Therefore, this metric not only measures smoothness but under some circumstances it can also measure fidelity, which is a more complex interpretation.

We propose the introduction of a new metric that considers, under the same index, the measurement of fidelity and smoothness, and at the same time the detection of how the two factors contribute to the global index. The index proposed is called the *global restoration index (GRI)* and is defined as the geometric mean of a fidelity and smoothing index, called *FI* and

$SI$  respectively. The geometric mean integration is performed between both indices to promote a good restoration method which supplies fidelity and smoothness in conjunction.

$$GRI = \sqrt{FI \cdot SI} \quad (7)$$

The *fidelity index* ( $FI$ ) is basically a mean absolute error exponent (8). The non-linear exponential function was introduced to increase the resolution for a better comparison among good techniques and to group the different techniques ranging from medium to significant residuals in the same non-valid category.

$$FI = e^{-\left(\sum_{i,j=1} |f(i,j) - \hat{f}(i,j)|\right) / \left(\sum_{i,j=1} 1\right)} \quad (8)$$

The *smoothing index* ( $SI$ ) is defined as the negative exponential of a rugosity factor  $\xi$  (9).

$$SI = e^{-\xi} \quad (9)$$

Defining the angular increments  $d\alpha$  in the x and y directions for the ideal  $f$  and estimated image  $\hat{f}$  in the following way

$$d\alpha_{fx} = \arccos \left( \frac{\vec{n}_f(i,j) \cdot \vec{n}_f(i-1,j)}{\|\vec{n}_f(i,j)\| \cdot \|\vec{n}_f(i-1,j)\|} \right) \quad (10)$$

$$d\alpha_{fy} = \arccos \left( \frac{\vec{n}_f(i,j) \cdot \vec{n}_f(i,j-1)}{\|\vec{n}_f(i,j)\| \cdot \|\vec{n}_f(i,j-1)\|} \right) \quad (11)$$

$$d\alpha_{\hat{f}x} = \arccos \left( \frac{\vec{n}_{\hat{f}}(i,j) \cdot \vec{n}_{\hat{f}}(i-1,j)}{\|\vec{n}_{\hat{f}}(i,j)\| \cdot \|\vec{n}_{\hat{f}}(i-1,j)\|} \right) \quad (12)$$

$$d\alpha_{\hat{f}y} = \arccos \left( \frac{\vec{n}_{\hat{f}}(i,j) \cdot \vec{n}_{\hat{f}}(i,j-1)}{\|\vec{n}_{\hat{f}}(i,j)\| \cdot \|\vec{n}_{\hat{f}}(i,j-1)\|} \right) \quad (13)$$

it is possible to define the rugosity factor with the following equation:

$$\xi = \left( \sum_{i,j=1} (d\alpha_{\hat{f}x} - d\alpha_{fx}) \cdot (d\alpha_{\hat{f}x} \geq d\alpha_{fx}) + (d\alpha_{\hat{f}y} - d\alpha_{fy}) \cdot (d\alpha_{\hat{f}y} \geq d\alpha_{fy}) \right) / \left( \sum_{i,j=1} 1 \right) \quad (14)$$

The rugosity,  $\xi$ , roughly measures a mean value of the normal angular changes in the restored image  $f$ , but doesn't consider the changes due to discontinuities. The conditional expression  $d\alpha_{\hat{f}} \geq d\alpha_f$ , serves to indicate that the changes in the normal vector are accumulated only over smooth surfaces and when there is a discontinuity, the condition fails and therefore no value is added.

The  $GRI$ ,  $FI$  and  $SI$  values are bounded by a 0 to 1 range, where 1 represents a perfect restoration and values close to 0 indicate poor quality restoration. In order to use the  $GRI$  index for comparison, it is necessary to generate a synthetic image, which will be used as the ideal reference. This reference will contain a representative set of features to be preserved. Since the absolute  $GRI$  value depends on the reference image employed, the absolute values obtained shouldn't be taken into account, whereas the relative differences among the tested filters should.

## 4 Evaluation: Filter performance comparison using the GRI index

Previously, we presented in figure 3 the restoration results of the  $3\sigma$ -MPF filter using a real image. Apparently, high smoothing and fidelity preservation was obtained. No more real images were tested because these experiments only give a visual impression of the performance, but it is not possible to give an objective conclusion using real images because the reference or ideal image is unknown. Therefore, for real images an index such as GRI, which needs the restored and the ideal image, cannot be used. In order to obtain a correct evaluation of the restoration methods, an objective index such as the recently defined *GRI* index should be used. In this section a performance comparison of eighteen restoration techniques is presented, using the *GRI* metric as the criterion to decide which method works better.

The eighteen techniques selected include linear, non-linear and non-iterative adaptive filters. The arithmetic mean and the gaussian filter were selected to represent linear filters; while in the non-linear class, the filters tested are the median, trimmed mean, mid-range, armonic and contra-armonic mean,  $Y_p$  and geometric mean, and a wavelet de-noising technique using soft thresholding with second order Daubechies masks. The adaptive methods included, which are expected to work better than the linear or non-linear filters since they are more sophisticated, are the sigma filter, contrast dependent outlier removal (CDOR), gradient inverse weight method (GIW), selected neighbourhood averaging filter (SNA), minimum mean square error (MMSE), multiresolution adaptive smoothing (MAS), double window-modified trimmed mean (DW-MTM), and of course, our  $3\sigma$ -MPF filter.

The test image, which act as the ideal reference for each restoration, is the one-dimensional profile displayed in figures 5a and 6a. This profile contains several typical shapes that represent almost all possible configurations in a real image, including step, crease and roof edges, as well as, flat, sloped and curved surfaces. The ideal test profile could be configured to match only the typical patterns for a particular application and under these circumstances selecting the most appropriate restoration technique using the GRI index. However, we considered it more interesting to create a test profile with enough patterns to achieve an application-independent evaluation.

The ideal reference profile was degraded with gaussian and a combination of gaussian and impulsive noise as can be seen in figures 5b and 6b. The *GRI* evaluation results for the eighteen methods when the profile is degraded with gaussian noise is presented in table 6 and some representative sample profiles are displayed in figure 5c-h. In the table the methods are sorted by decreasing *GRI* index. To understand better how this filter works, the fidelity and smoothing factors are also presented. Since the profiles have a reduced size and could generate GRI values with certain dispersions due to particular noise configurations, the index values are averaged over one hundred profiles. As it was expected, the adaptive filters obtained the best results, the  $3\sigma$ -MPF filter being the most significant showing a high fidelity ( $FI=0.64$ ) and an exceptional smoothing ( $SI=0.87$ ). Consequently, it is given a global index, *GRI*, of 0.75. In a second plane, the DW-MTM filter and the MAS method also demonstrate high fidelity indices (0.62 and 0.61), however the smoothing obtained (0.76) is far from that obtained with our filter. It should be noted that when using the *GRI* index we obtained the same results previously presented by Lee<sup>(7)</sup>, i.e. the sigma filter performs better against gaussian noise than the Median, SNA and GIW filters with 0.65, 0.61, 0.57, 0.55 *GRI* indices respectively.

Exactly the same process was repeated but in this case with a combination of gaussian and impulsive noise. A 4% outlier degraded sample is shown in figure 6b and six representative restored profiles, for a visual impression, in figures 6c-h. Additionally, one of the best outlier

removing filters, i.e the median filter ( $GRI=0.91$  with only outliers) was used as a first step in two dual-stage filters, applying the MAS and DW-MTM methods in the second steps. The idea was to increase the MAS and DW-MTM performance removing the outliers to facilitate the filtering process, especially for the MAS filter which is not robust against outliers. In table 6 the methods ordered by the  $GRI$  index are presented. It can be seen that there is an improvement using the two step filters when compared with the MAS and DW-MTM working alone. The results are not outstanding because the fidelity degradation introduced in each step was added. On the other hand, the  $3\sigma$ -MPF filter ( $GRI=0.69$ ), although slightly affected by the outliers because over these pixels the smoothing reached is not very high, exhibits a strong tendency to reject the outliers and performs slightly better than others filters ( $GRI$  below 0.68).

The visual correspondence should be noted between the restored profiles displayed in figures 5 and 6 with the  $GRI$ ,  $FI$  and  $SI$  values obtained. A good example is the gaussian profile in figure 5c where the smoothing obtained is visually high ( $SI=0.77$ ) and the step edges which appeared rounded were not preserved ( $FI=0.30$ ). The opposite case occurs in the wavelet profile in figure 5d, where the visual smoothing is poor ( $SI=0.67$ ) and the preservation apparently is better than in the gaussian case ( $FI=0.54$ ).

## 5 Conclusions

This paper presented a new restoration filter ( $3\sigma$ -MPF) specially designed to achieve accurate and smooth restorations, a global restoration index ( $GRI$ ) to evaluate filter performances, and a very interesting comparison between eighteen filters. The proposed  $3\sigma$ -MPF restoration method obtained the best grades when eliminating Gaussian noise. This filter is characterized and differs from other methods because it does not require user specified parameters such as threshold values and does not compare local homogeneity statistics with global estimates to obtain adaptive behavior decisions which can be erroneous since small windows usually are not appropriate samples to compute statistics. The filter does not require multiple iterations, therefore the complexity of the algorithm is limited by  $O(N \times M)$  where  $N \times M$  is the size of the image.

The outstanding results obtained by the  $3\sigma$ -MPF filter are based on the multiresolution approach and reliable detection of discontinuities which are both controlled by the plane fitting  $3\sigma$ -fidelity test, which also serves to detect outliers which are finally rejected by the MTM filter. The filter only requires the estimation of the global additive noise degradation affecting the image which can be computed in a robust manner by the variance histogram mode detection proposed by Meer<sup>(11)</sup> which assures a reliable estimation since the edges are mapped into long distribution tails.

The proposed global restoration index,  $GRI$ , is based on an ideal model consisting of smooth continuous regions separated by discontinuities and measures both fidelity and smoothness. This metric is a better estimation of the final restoration quality obtained because it does not only consider the pixel to pixel deviation, but also the distribution inside a region. There is a necessity to use a standard index to measure restoration qualities and the  $GRI$  metric includes enough features to be considered as a serious candidate.

## 6 Acknowledgments

The authors acknowledge the financial support of the Spanish Commission for Science and Technology (CICYT) under the TAP-583/93 and TAP-398/96 projects. Special thanks to Prof.

John Illingworth for the advice and facilities supplied at the CVSSP centre (Surrey University-U.K) where part of this work was done.

## Bibliography

1. W. K. Pratt. *Digital Image processing*. Wiley, (1991).
2. P.M. Clarkson and G.A. Williamson. Order statistics and adaptive filtering. *Signal processing methods for audio, images and telecommunication*, pages 109–141, (1995).
3. R.M. Haralick and L.G. Shapiro. *Computer and robot vision*, volume 1. Addison Wesley, (1992).
4. R.R. Coifman and D. Donoho. Translation-invariant de-noising. *Wavelets and Statistics*, pages 125–150, (1995).
5. D. Greenhill and E.R. Davies. Relative effectiveness of neural networks for image noise suppression. *Pattern recognition in Practice*, 4:367–378, (1994).
6. J. Varona and J.J. Villanueva. Neural networks as spatial filters for image processing: Neurofilters. *CVC Tech. Report no. 007*, pages 1–11, (1996).
7. J.S. Lee. Digital image smoothing and the sigma filter. *Computer Vision, Graphics and Image processing*, 24:255–269, (1983).
8. J.S. Lee. Digital image enhancement and noise filtering by use local statistics. *IEEE Trans. on Pattern Recognition and Machine Intelligence*, 2:165–168, (1980).
9. J.S. Lee. Refined filtering of image noise using local statistics. *Computer graphics and image processing*, 15:380–389, (1981).
10. A.P. Witkin. Scale-space filtering. *IEEE Computer Society Press. Computer Vision: Principles*, pages 108–111, (1991).
11. P. Meer, R. Park, and K. Cho. Multiresolution adaptive image smoothing. *CVGIP: Graphical Models and Image processing*, 56(2):140–148, (1994).
12. P. Saint-Marc, J.L. Jezonin, and Medioni. A versatile pc-based range finding system. *IEEE Transactions on Robotics and Automation*, 7(2), (1991).
13. P. Perona and J. Malik. Scale space and edge detection using anisotropic diffusion. *IEEE Trans. Int. Conf. PAMI*, 12:629–639, (1990).
14. H.R. Myler and A. R. Weeks. *The pocket handbook of image processing algorithms in C*. Prentice Hall, (1993).
15. R.M. Haralick and L. Watson. A facet model for image data. *Computer Graphics Image Processing*, 15:113–129, (1981).
16. P. Saint-Marc, J. Chen, and G. Medioni. Adaptive smoothing: A general tool for early vision. *IEEE Transactions on pattern Analysis and Machine Intelligence*, 13(6):514–529, (1991).
17. X. Yu, D. Bui, and A. Krzyzak. Robust estimation for range image segmentation and reconstruction. *IEEE Trans. Pattern Analysis and Machine Intelligence*, 16(5):530–537, (1994).
18. E. Trucco. On shape-preserving boundary conditions for diffusion smoothing. *IEEE International conference on Robotics and Automation. Nice, France*, pages 1690–1694, (1992).
19. M. Umasuthan and A.M. Wallace. Outlier removal and discontinuity preserving smoothing of range data. *IEE Proceeding Vis. Image Signal Process.*, 143(3):191–200, (1996).
20. A.R. Jiménez, R. Ceres, and J.L. Pons. Shape-based methods for fruit recognition and localization using a laser range-finder. *Bio-Robotics-97. International Workshop on robotics and automated machinery for bio-productions*, (1997).

21. R. Ceres, J.L. Pons, A.R. Jiménez, J.M. Martín, and L. Calderón. Agribot: A robot for aided fruit harvesting. *AgENG96-Paper 96A-107*, (1996).

## BIOGRAPHIES

Antonio R. Jiménez graduated in Physics, Computer Science branch (Universidad Complutense of Madrid, June 1991). He received the Ph. D. degree in physics sciences from the Complutense University of Madrid, October 1998. From 1991 to 1993, he worked in industrial laser applications at CETEMA (Technological Center of Madrid), Spain. From 1994, he is working as research assistant at the Instituto de Automática Industrial, CSIC, Spain. His current research interests include computer vision applications, pattern recognition, range images, shape-based image analysis and automatic harvesting.

Ramón Ceres graduated in Physics (electronic) from Universidad Complutense of Madrid in 1971 and received the doctoral degree in 1978. After a stay of one year, in the LAAS-CNRS in Toulouse (France), has been working at the Instituto de Automática Industrial (IAI), dependent of the Spanish National Council for Science Research; excluding a one year position in an electronic company (Autelec) as R&D director. As a researcher, Dr Ceres has worked on sensor systems for different fields such as continuous process control, machine tool, agriculture, robotics and disable people. On these topics has more than seventy papers and congress presentations, and has several patents in industrial use. At present Dr Ceres is the Spanish delegate for the IMT (Brite-Euram) Committee and Deputy Scientific Director of the IAI.

José L. Pons graduated as Mechanical Engineering (Universidad de Navarra, April 1992). He received a M. Sc. degree in Information Technologies for Production (Universidad Politécnica de Madrid, January 1995). He received the Ph. D. degree in physics sciences from the Complutense University of Madrid, December 1996. Dr. Pons is currently at the Instituto de Automática Industrial, CSIC, where has been working from 1993. His current research interests include non-traditional sensor-actuation technologies, development of new technologies and miniature applications.

Figure 1. Pseudocode for the  $3\sigma$ -MPF adaptive filter.

Figure 2. Restoration of synthetic images with gaussian, impulsive and a combination of both types of noise using the  $3\sigma$ -MPF filter.

Figure 3. Range image restoration using the  $3\sigma$ -MPF filter.

Figure 4. Masks showing the adaptive behaviour of  $3\sigma$ -MPF when filtering the image in figure 3.

Figure 5. Test, noisy and restored profiles for gaussian degradation. In parenthesis:  $GRI$ ,  $FI$  and  $SI$  indices.

Figure 6. Test, noisy and restored profiles for impulsive plus gaussian degradation. In parenthesis:  $GRI$ ,  $FI$  and  $SI$  indices.

For each image pixel  $g(i,j)$

$\sigma$ =noise\_estimation( $g(i,j)$ );

window\_size=7x7;

REPEAT

a,b,c=least\_square\_plane\_fitting( $g(i,j)$ ,window\_size);  
 $3\sigma$ \_fidelity\_test= $3\sigma$ \_fidelity( $g(i,j)$ ,window\_size,(a,b,c), $\sigma$ );  
 IF  $3\sigma$ \_fidelity\_test==FALSE  
     window\_size=window\_size-2x2;

UNTIL ( $3\sigma$ \_fidelity\_test==TRUE OR window\_size<3x3);

IF  $3\sigma$ \_fidelity\_test==TRUE // continuous region found

$\hat{f}(i,j)=c$ ;

ELSE // discontinuity or outlier detected

ref=Median( $g(i,j)$ ,3x3,4\_connectivity);  
 $\hat{f}(i,j)=3\sigma$ \_range\_mean( $g(i,j)$ ,3x3,8-connectivity,| $g(x,y)$ -ref|<3 $\sigma$ )

END

Figure 1:

Restoration method	<i>GRI</i>	<i>FI</i>	<i>SI</i>
<b>3<math>\sigma</math>-MPF</b>	<b>0.75</b>	<b>0.64</b>	<b>0.87</b>
DW-MTM (window side=3,5)	0.69	0.62	0.76
MAS (w.s.=7,5,3)	0.68	0.61	0.76
MMSE (w.s.=3)	0.66	0.59	0.74
Sigma (w.s.=5)	0.65	0.61	0.70
Median (w.s.=3)	0.61	0.57	0.66
Wavelet	0.60	0.54	0.67
SNA (w.s.=3)	0.57	0.52	0.64
GIW (w.s.=5)	0.55	0.56	0.54
Trimmed mean (w.s.=5, mean w.s.=3)	0.50	0.32	0.79
Arithmetic mean (w.s.=3)	0.49	0.37	0.65
Geometric mean (w.s.=3)	0.49	0.36	0.65
$Y_p$ mean (w.s.=3, power=2)	0.48	0.36	0.65
Gaussian (w.s.=7)	0.48	0.30	0.77
Armonic mean (w.s.=3)	0.48	0.35	0.65
Contra-armonic (w.s.=3, power=2)	0.45	0.31	0.66
CDOR (w.s.=5, Threshold=5)	0.44	0.47	0.42
Mid-Range (w.s.=5)	0.32	0.15	0.68

Table 1: Restoration evaluation using the *GRI* index for gaussian noise.

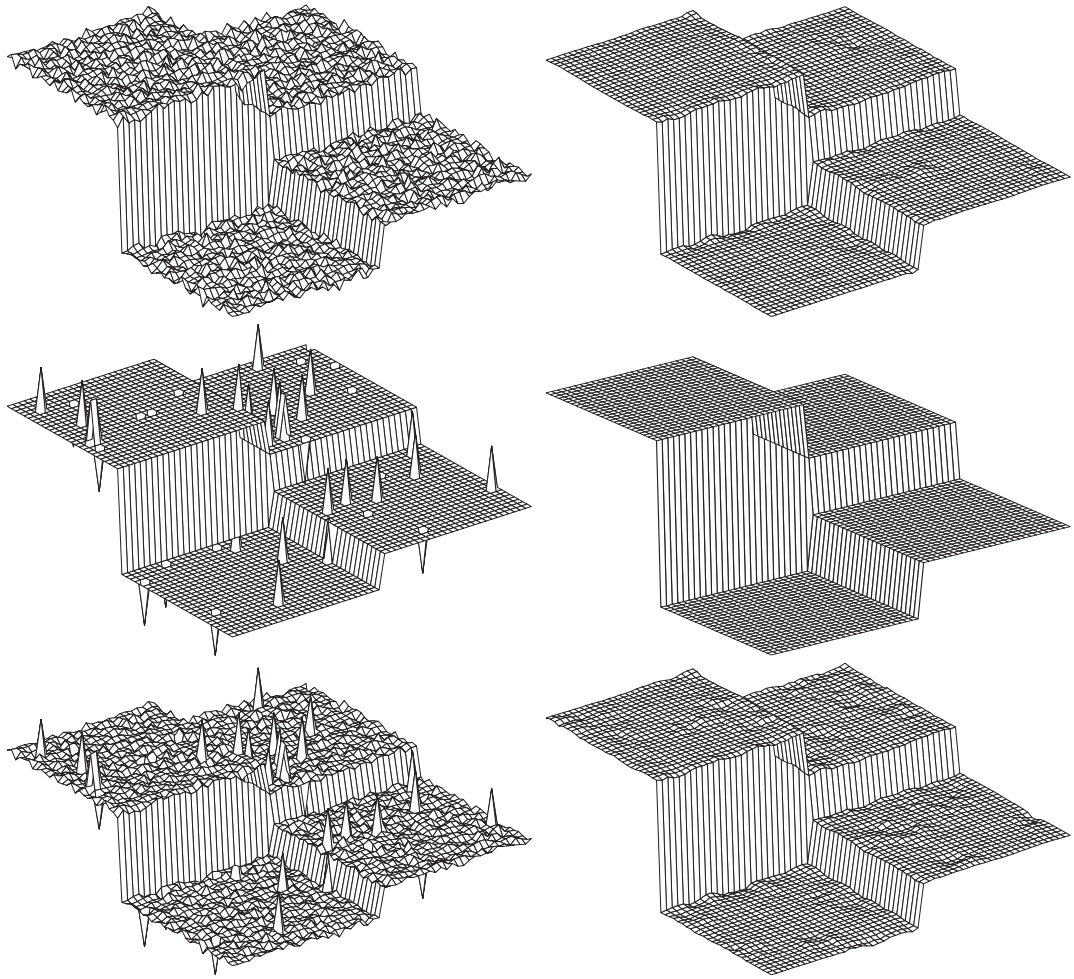


Figure 2:

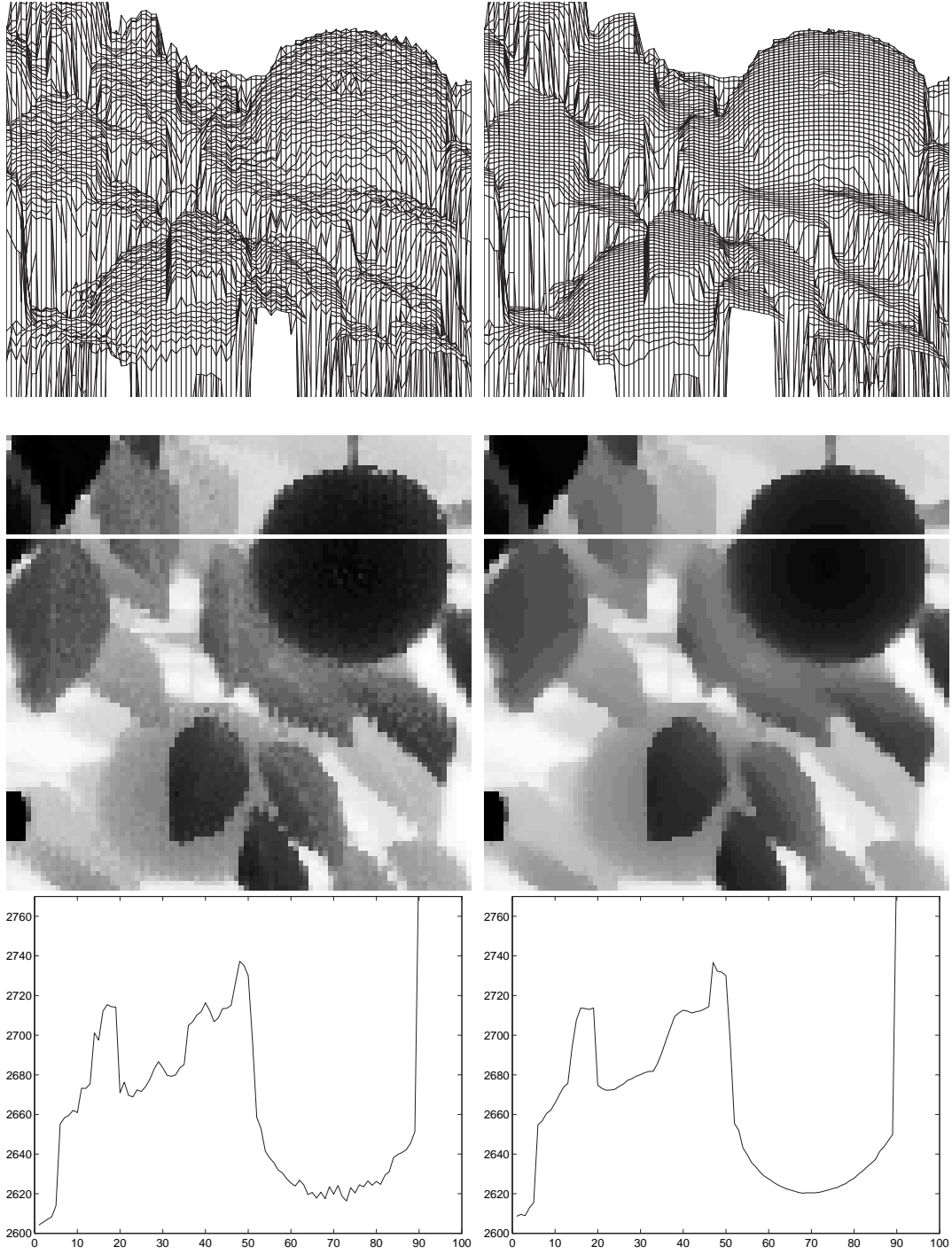


Figure 3:

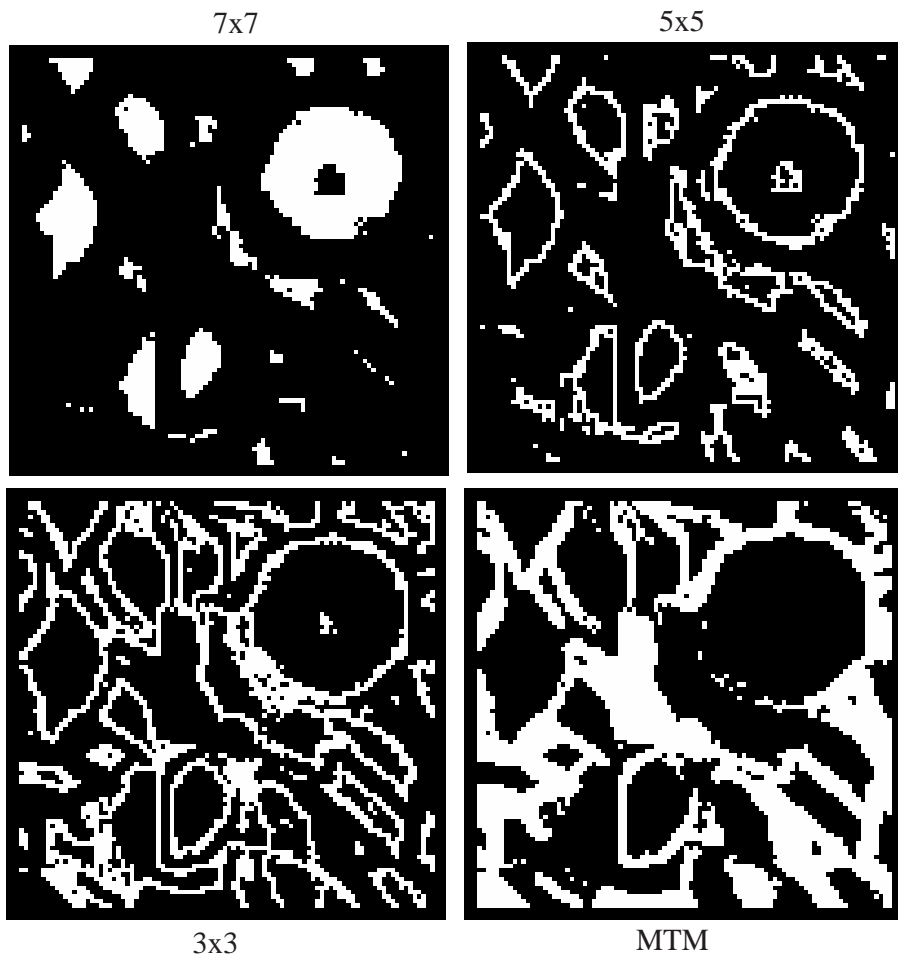


Figure 4:

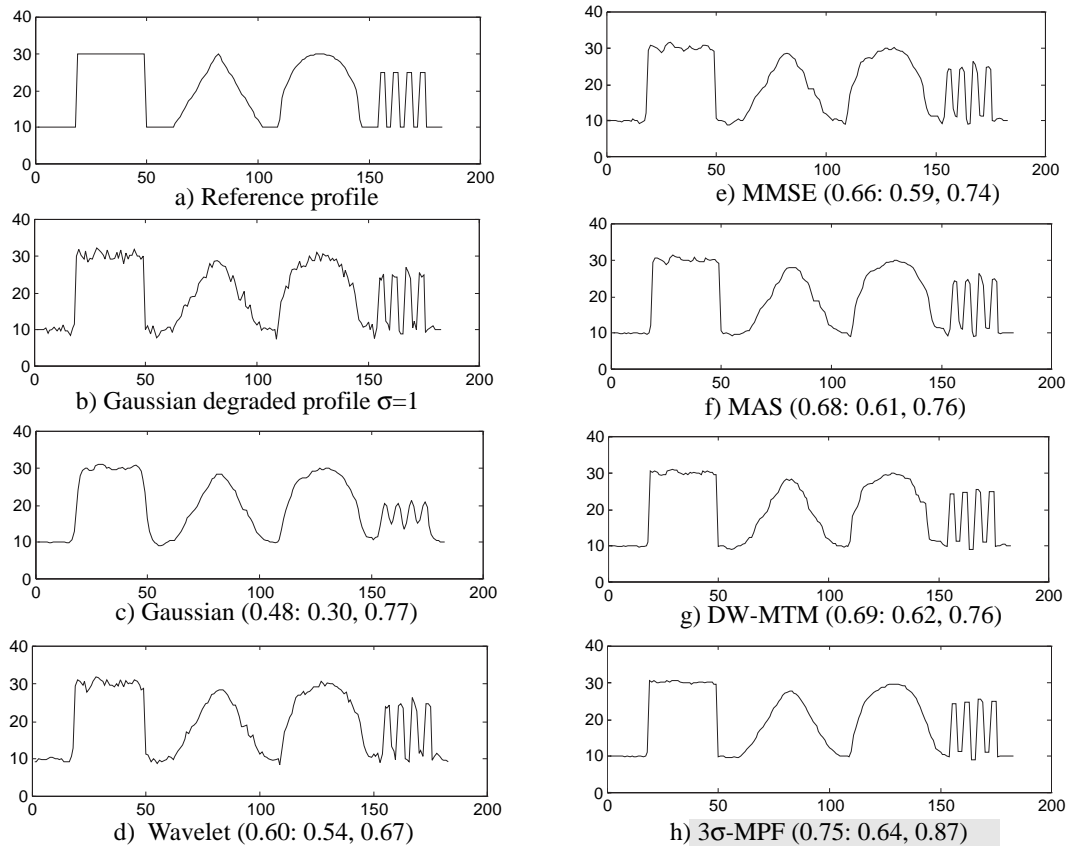


Figure 5:

Restoration method	<i>GRI</i>	<i>FI</i>	<i>SI</i>
<b>3<math>\sigma</math>-MPF</b>	<b>0.69</b>	<b>0.58</b>	<b>0.82</b>
Median + DW-MTM	0.68	0.55	0.83
Median + MAS	0.67	0.55	0.82
DW-MTM (window side=3,5)	0.65	0.56	0.75
Median (w.s.=3)	0.57	0.51	0.64
Trimmed mean (w.s.=5, mean w.s.=1)	0.46	0.29	0.75
CDOR (w.s.=5, Threshold=5)	0.44	0.46	0.42
SNA (w.s.=3)	0.37	0.25	0.56
Geometric mean (w.s.=3)	0.34	0.19	0.59
GIW (w.s.=5)	0.32	0.21	0.47
MAS (w.s.=7,5,3)	0.24	0.09	0.63
MMSE (w.s.=3)	0.23	0.09	0.62
Sigma (w.s.=5)	0.23	0.09	0.59
$Y_p$ mean (w.s.=3, power=2)	0.21	0.07	0.59
Gaussian (w.s.=7)	0.20	0.06	0.68
Wavelet	0.20	0.08	0.49
Arithmetic mean (w.s.=3)	0.18	0.06	0.57
Contra-armonic (w.s.=3, power=2)	0.08	0.01	0.57
Mid-range (w.s.=5)	0.04	0.002	0.59
Armonic mean (w.s.=3)	0.03	0.001	0.57

Table 2: Restoration evaluation using the *GRI* index for impulsive and gaussian noise.

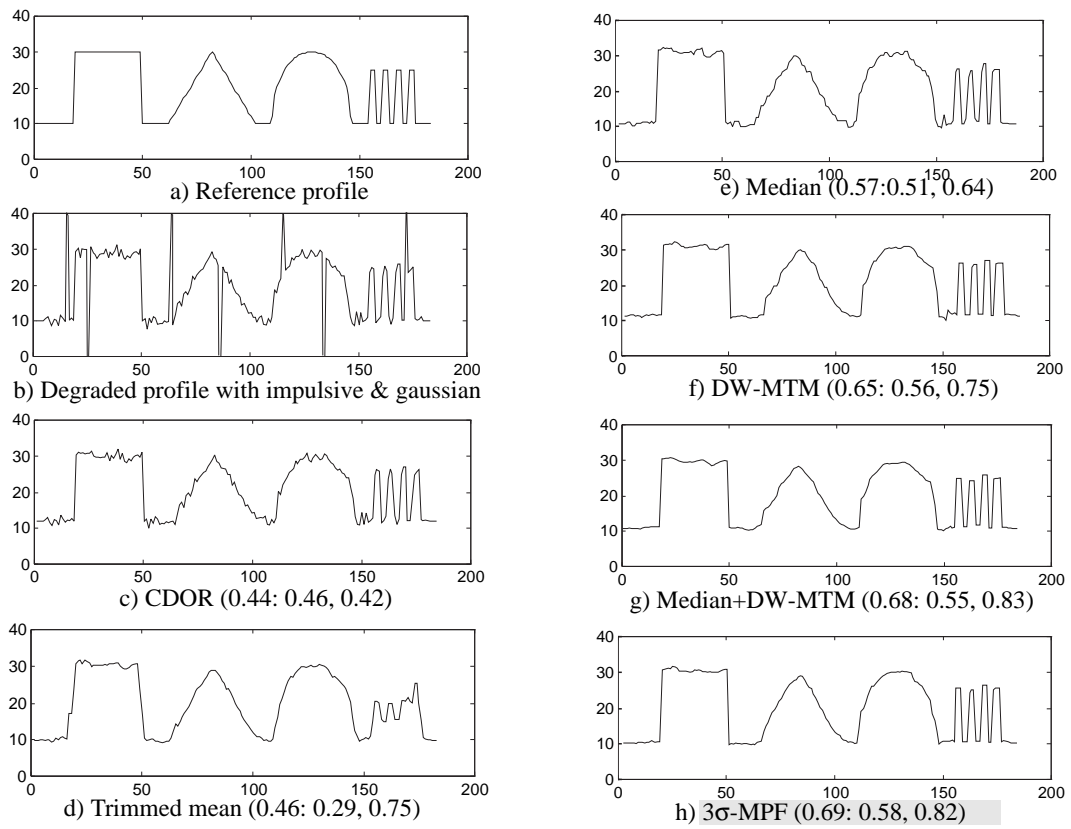


Figure 6: